Supplementary Methods

Enzyme expression and purification

The expression vector pJEL236 (18) encoding the full length *S. cerevisiae* topoisomerase II enzyme fused to an intein and a chitin binding domain was kindly provided by Janet Lindsley, University of Utah. A secondary mutation (A3925G) was reverted to the wild-type sequence by QuickChange site directed mutagenesis (Stratagene) after subcloning the coding sequence into pBluescript II KS+ (Fermentas). In addition, a Y782F mutation was introduced by QuickChange mutagenesis. The coding sequences were cloned back into the pJEL236 vector backbone. A kanamycin resistence gene was inserted into the Apa1 site to yield pFMP54 encoding wild-type and pFMP69 encoding the Y782F mutant topoisomerase. The DNA sequences were verified by DNA sequencing of the full coding regions. The constructs were designed such that the only difference between *S. cerevisiae* topoisomerase II and the final, purified topoisomerase is a change of the C-terminal aspartic acid is to glycine. Purified protein with this one change was reported to have identical biochemical characteristics to the fully wild-type enzyme (18); for the purposes of these studies, it is referred to as wild-type topoisomerase II.

Single colonies of the yeast expression strain BCY123 harboring pFMP54 or pFMP69 were grown in YP-Raffinose in the presence of 0.2 mg/mL G418 (A.G. Scientific). Cells were induced and harvested as described (18) and stored at -80 ˚C. To purify topoisomerase II, cells were lysed in liquid nitrogen using a Waring blender. Chitin affinity chromatography was performed essentially as described (18). Intein cleavage was induced with 30 mM DL-dithiothreitol (Sigma) overnight at 4 ˚C in FPLC buffer [50 mM potassium HEPES pH 7.5, 20% sucrose, 0.1 mM EDTA, 0.01% Tween 20] plus 500 mM potassium acetate (KOAc). Protein containing fractions from the elution were diluted 1:1 with FPLC buffer + 100 mM KOAc and loaded on a Heparin FF column (Pharmacia) from which topoisomerase II was eluted with a KOAc gradient (0.25 to 0.7 M). Topoisomerase-containing fractions were loaded undiluted on a MonoQ (Pharmacia) column and eluted with a KOAc gradient (0.5 to 1 M). The most concentrated fractions were pooled and further concentrated to 10-30 μM using an Amicon Ultra (Millipore) 100K cutoff centrifugal filter. The concentrate was aliquoted and stored at -80 ˚C. Per 40 g of wet weight cells (from ~8 L culture), the yield was 5 mg for wild-type and 1 mg for Y782F topoisomerase II. The purity was ≥95% based on Coomassie Blue staining of SDS gels (Supplementary Figure S1 and data not shown). Topoisomerase II can be reversibly phosphorylated. The phosphorylation state of the enzyme was not monitored or controlled.

Selection of the DNA duplex for the DNA cleavage assay

Topoisomerase-mediated cleavage of the 40 bp and 68 bp duplex substoichiometric with respect to enzyme in the presence of Mg^{2+}-AMPPNP could be detected, but the signal was too low for accurate quantification (<1%; data not shown). A series of duplexes with palindromic sequences was created based on the cleavage site within the 40 bp duplex (unpublished results). The lengths of these duplexes were increased to 46 bp to position the cleavage site in the center of the DNA. The sequence providing the highest extent of cleavage was selected for the cleavage experiments herein (Supplementary Table S1). The cleavage specificity of the main cleavage site of the 46 bp duplex used in this study was >95% (data not shown).

ATPase assay

ATP hydrolysis was measured by a coupled ATPase assay using pyruvate kinase (15 U/mL final concentration), PEP (6 mM), lactate dehydrogenase (15 U/mL), NADH (0.5 mM) and varying concentrations of Mg^{2+}-ATP in 0.1 mL reactions. The absorption of NADH over time was read by a SpectraMax 340 PC 96 well plate reader in flat bottom, uncoated 96 well plates (Nunc). ATP resynthesis apparently did not limit the measured rates: varying the ATP regenerating system concentration two-fold did not result in changes of the measured rates. This result is corroborated by control experiments in which the solution containing the ATP regenerating system was mixed with pure ADP. Rates for ATP regeneration in those experiments were at least five times faster that the rates in experiments containing topoisomerase II. Individual ATPase activities between independent experiments varied on average 7% (standard error) for saturating (3 mM) and 15% for subsaturating (0.06 mM) ATP concentrations.

Supplementary Results

Models to account for the biphasic DNA stimulation of the ATPase activity of the Y782F topoisomerase II

Three limiting models can account for the observed biphasic DNA stimulation curve of the Y782F enzyme (Supplementary Scheme 3). The first model was presented in the main text and is shown in the Supplementary Scheme 3A for comparison. According to this model, binding of DNA to the higher affinity binding site (defined as K_d^1; the thickness of the red arrows indicates the relative affinities of different enzyme species for DNA) partially stimulates ATP hydrolysis. Increased ATP hydrolysis is indicated by thicker, blue arrows in Supplementary Scheme 3. This model implies communication between each DNA binding site and the ATPase activity, as binding of each DNA activates ATP hydrolysis. The modest level of stimulation observed from binding of the first DNA to the mutant enzyme would not be expected to be detectable in the analogous experiment with the wild-type enzyme, as the affinities for the first and second DNAs are not sufficiently different in the wild-type. Thus, the results with the wild-type enzyme do not provide evidence for this model but are fully consistent with it (Supplementary Figure S2).

A second model to explain the biphasic stimulation curve does not require that DNA bound at the higher affinity site partially activates ATP hydrolysis. The ATPase activity is stimulated only in complexes that have the lower affinity site occupied (E_{DNA_2} and $E_{DNA_2}^{DNA_1}$; Supplementary Scheme 3B). To obtain measurable ATPase stimulation by binding of a single DNA in this model, a significant fraction of DNA would have to be bound to the lower affinity site under conditions when the enzyme is in excess of DNA (i.e. $K_d^1 \sim K_d^2$). The dissociation constant for the second DNA to bind to the mutant enzyme is significantly larger than that for the first DNA [$K_d^1 < 1$ nM (Scheme 1), $K_d^{2'} \geq 550$ nM (Table II) and data not shown]. Consequently, the model requires that DNA binding exhibits negative binding cooperativity ($K_d^2 < K_d^{2'}$): i.e., G-DNA binding would inhibit binding of T-DNA and vice versa. However, negative binding cooperativity of more than three-fold is not consistent with ATPase activity results for the wild-type enzyme under identical conditions (Supplementary Figure Supplementary Figure S3C). Thus, the Y782F mutation would have to induce negative DNA binding cooperativity not present in the wild-type enzyme for this model to hold.

A third model requires that the enzyme species with DNA bound only at the lower affinity site (E_{DNA_2}) have a hyperstimulated ATPase activity compared to the other enzyme species (Supplementary Scheme 3C). Even though E_{DNA_2} cannot strongly accumulate in this model due to unfavorable DNA affinities ($K_d^1 << K_d^2$) , the small fraction of E_{DNA_2} formed with enzyme in excess of DNA would be sufficient to significantly stimulate the observed ATPase activity. Quantitative analysis shows that the ATPase activity of E_{DNA_2} would have to be stimulated >1000-fold compared to free enzyme to fit the data (analysis not shown). Because the overall DNA stimulation of the ATPase activity at saturating DNA concentrations is only ~20-fold compared to DNA free enzyme, binding of the second DNA segment would then have to inhibit DNA stimulation by at least 50-fold. As in the first model described above, this model requires communication between both DNA binding sites and the ATPase activity except that in this model DNA_2 in the $E_{DNA_2}^{DNA_1}$ -complex is stimulatory and DNA_1 is inhibitory to the ATPase activity. This model, like the first, is consistent with data obtained with the wild-type enzyme (data not shown).

In summary, models 1 and 3 require that both DNA binding sites can communicate with the ATPase domains. While in model 1 each DNA partially activates ATP hydrolysis, model 3 postulates one inhibitory and one stimulatory binding site. In contrast, model 2 demands that only one of the DNA binding sites is stimulatory to the ATPase activity. Model 2 requires that the Y782F mutation induces negative DNA binding cooperativity between the two binding sites, and model 3 requires that a hyperstimulated ATPase state exists. We adopt the first model (Supplementary Scheme 3A) as our working model due to its simplicity, its consistency with the DNA-dependent ATPase stimulation for the wild-type enzyme, and the lack of a requirement for additional *ad hoc* assumptions.

Alternative models accounting for the DNA dependence of DNA cleavage

As described in the main text, the DNA dependence of DNA cleavage is consistent with a model that does not require the presence of a bound T-segment before the G-segment can be cleaved. Two alternative models could in principle also account for the data, but they can be rejected based on data presented herein and additional unpublished results, as described below.

First, DNA binding could be strongly cooperative, such that under the conditions employed the enzyme would never be significantly bound to only a single DNA (Supplementary Scheme 4; thickness of arrows indicates the relative affinities). In this case, it would not be

possible to distinguish if the T-segment were required allosterically for cleavage. However, at most 50% of the DNA could be cleaved in this scenario because at most 50% of the DNA segments could be bound at the G-DNA site. Thus, this model could only explain the DNA cleavage data obtained in Mg^{2+} where <10% cleavage is observed, but is not consistent with the >80% DNA cleavage observed in Ca^{2+}. A quantitative analysis of the data showed that binding of the second segment in Mg^{2+} would have to occur with a $\geq 10^4$-fold higher affinity than binding of the first ($K_d^{T'} \leq K_d^G / 10^4$ and $K_d^{G'} \leq K_d^T / 10^4$, i.e., with 10^4-fold observed binding cooperativity; Supplementary Figure S6 and data not shown). However, the analysis of the dependence of ATPase hydrolysis on the concentration of the 40 bp and 68 bp duplexes indicates that there is no observed binding cooperativity (Table II). Differences between the DNA cleavage assay conditions compared to the ATPase assay conditions are not responsible for inducing observed cooperativity*. Thus, a model requiring strong, positive observed cooperativity to explain the DNA cleavage results can be rejected.

In a second alternative model, DNA could bind transiently at the T-DNA binding site and induce cleavage of a bound G-DNA. The DNA at the T-DNA site could then dissociate and bind to the T-DNA site of another enzyme molecule promoting cleavage and so forth. This possibility can be ruled out based on unpublished kinetic results, as follows. Microscopic reversibility would require that T-DNA also be required for ligation of cleaved DNA at the G-DNA site. However, DNA religation by topoisomerase II followed in pulse-chase type experiments in which ligation is induced by adding in a large excess of unlabeled DNA or by diluting the reaction mixture give the same rate constant for ligation (unpublished results). These results indicate that a second, transiently bound DNA is not involved in establishing the cleavage/ligation equilibrium.

*A 46 bp duplex was employed in the DNA cleavage assay while a 40 bp and a 68 bp duplex were used in the ATPase assay opening the possibility that the specific length or sequence of the 46 bp duplex could promote observed binding cooperativity. The observation of DNA cleavage in Mg^{2+}, Mg^{2+}-AMPPNP, Ca^{2+} and Ca^{2+}-AMPPNP for the 40 bp and 68 bp DNA duplexes under conditions where the enzyme was in large excess of DNA provides evidence against that possibility (data not shown). Furthermore, it is possible that AMPPPNP used in the DNA cleavage assay induces observed binding cooperativity. Evidence against that possibility comes from the observation that DNA cleavage of the 40 bp, 46 bp and 68 bp duplexes was detected also in the absence of AMPPNP in Mg^{2+} with the enzyme concentration in large excess of the DNA concentration (data not shown). Finally, the presence of bound ATP in the ATPase assay may prevent observed DNA binding cooperativity. However, the analysis of the ATPase data indicated the absence of observed DNA binding cooperativity also under subsaturating ATP conditions (Table II).

Table S1 Oligodeoxyribonucleotides used in this study

Name	**Sequence (5' – 3')**
$Oligo_{68}$top	GCTAACGCAGTCAGGCACCGTGTATGAAATCTAACAATGCGCTCATCGTCATCCTCGGCACCGTCACC
$Oligo_{68}$bottom	GGTGACGGTGCCGAGGATGACGATGAGCGCATTGTTAGATTTCATACACGGTGCCTGACTGCGTTAGC
$Oligo_{40}$top	TGAAATCTAACAATGCGCTCATCGTCATCCTCGGCACCGT
$Oligo_{40}$bottom	ACGGTGCCGAGGATGACGATGAGCGCATTGTTAGATTTCA
$Oligo_{40}$top-ROX [a]	ROX-TGAAATCTAACAATGCGCTCATCGTCATCCTCGGCACCGT
$Oligo_{46}$ [b]	ACGGTGCCGAGGATGACGATGCGCGCATCGTCATCCTCGGCACCGT

[a] ROX: 6-Carboxy-X-rhodamine.

[b] $Oligo_{46}$ is self-complementary, so top and bottom strands are identical.

Supplementary Scheme 3

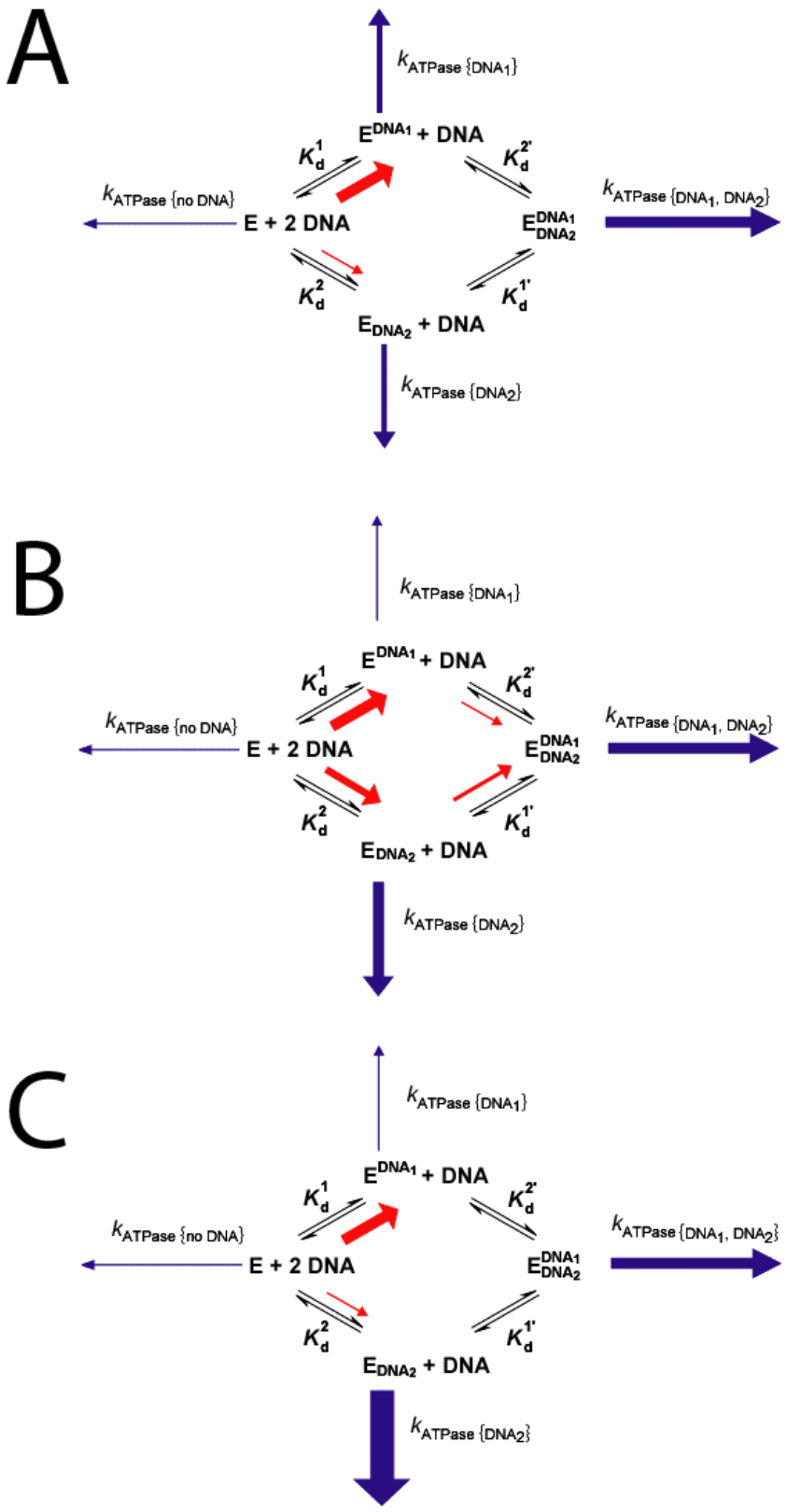

Supplementary Scheme 4

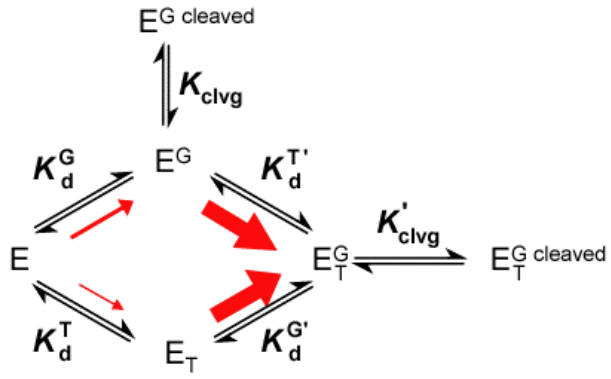

Supplementary Figures

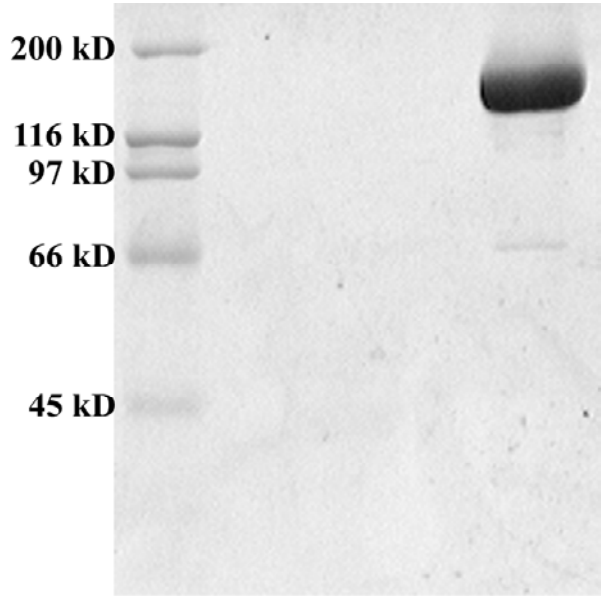

Supplementary Figure S1: Assessment of the purity of the topoisomerase II preparation. Purified wild-type topoisomerase II (~1 μg; theoretical molecular weight 164 kD) was analyzed on a 10% SDS polyacrylamide gel and stained with Coomassie Blue. Quantification of bands in the gel indicates a purity of ≥95% of the topoisomerase II preparation.

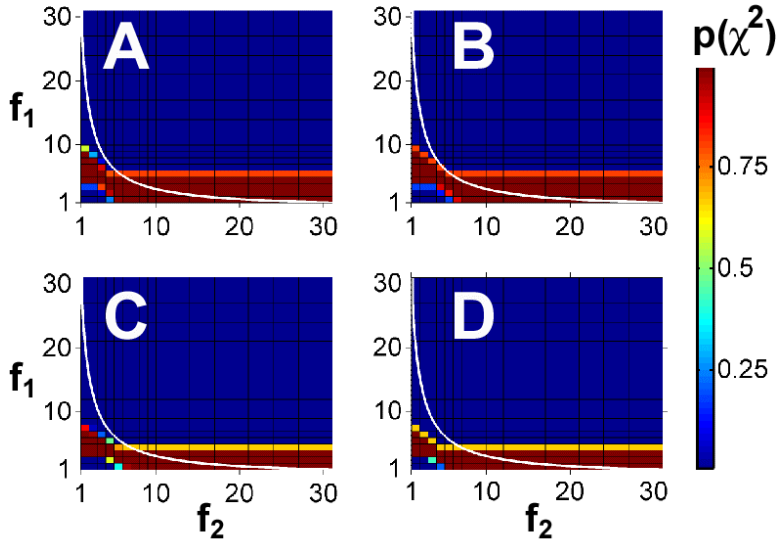

Supplementary Figure S2: Range of ATPase stimulation that can be elicited by each bound DNA segment in the absence of the other. The DNA stimulation curves of the ATPase activity at saturating ATP concentrations from Figure 2A were fit to a set of models with ATPase activities for E and $E_{DNA_2}^{DNA_1}$ fixed at the levels observed in the absence of DNA and the presence of saturating DNA, respectively, but varied in the level of the ATPase activity for E^{DNA_1} and E_{DNA_2} (Scheme 1). The ratio between the ATPase activity of E^{DNA_1} and E is defined as f_1, and f_2 is similarly defined as the ratio of the ATPase activities of E_{DNA_2} and E. The probability $p(\chi^2)$ that a particular model can fit the data was estimated based on a chi square goodness-of-fit test. K_d^2 in the fits is defined to be of equal or greater value than K_d^1 ($K_d^2 \geq K_d^1$) as it refers to the weaker binding site. $p(\chi^2)$ is plotted over a plane defined by f_1 and f_2. Different ranges of values for $p(\chi^2)$ are assigned different colors. Models with a low probability to fit the data based on the χ^2 test are assigned a blue color (see color bar). To fit the data, K_M^{ATP} values for all four enzyme species are needed (see Experimental Procedures), but only the K_M^{ATP} values for free enzyme (E, $K_{M\{\text{no DNA}\}}^{ATP} = 1$ mM) and $E_{DNA_2}^{DNA_1}$ ($K_{M\{DNA_1,DNA_2\}}^{ATP} = 0.2$ mM; Table I) are known. Four permutations of K_M^{ATP} values of E^{DNA_1} and E_{DNA_2} that span the values for E and $E_{DNA_2}^{DNA_1}$ were considered: A) $K_{M\{DNA_1\}}^{ATP} = K_{M\{DNA_2\}}^{ATP} = 1$ mM. B) $K_{M\{DNA_1\}}^{ATP} = 1$ mM and $K_{M\{DNA_2\}}^{ATP} = 0.2$ mM. C) $K_{M\{DNA_1\}}^{ATP} = 0.2$ mM and $K_{M\{DNA_2\}}^{ATP} = 1$ mM. D) $K_{M\{DNA_1\}}^{ATP} = K_{M\{DNA_2\}}^{ATP} = 0.2$ mM. Values for

$K_{M\{DNA_1\}}^{ATP}$ and $K_{M\{DNA_2\}}^{ATP}$ below 0.2 mM or above 1 mM are possible. K_M^{ATP} values below 0.2 mM would not change the conclusions because ATP remains saturating for all species. Values significantly above 1 mM would prevent ATP from being saturating for the particular species; the ATPase activity of this species would still be stimulated by DNA but the reported stimulation would be an underestimate. The white line indicates the position of models for which the product of f_1 and f_2 totals the maximal stimulation observed at saturating DNA concentrations of 31-fold.

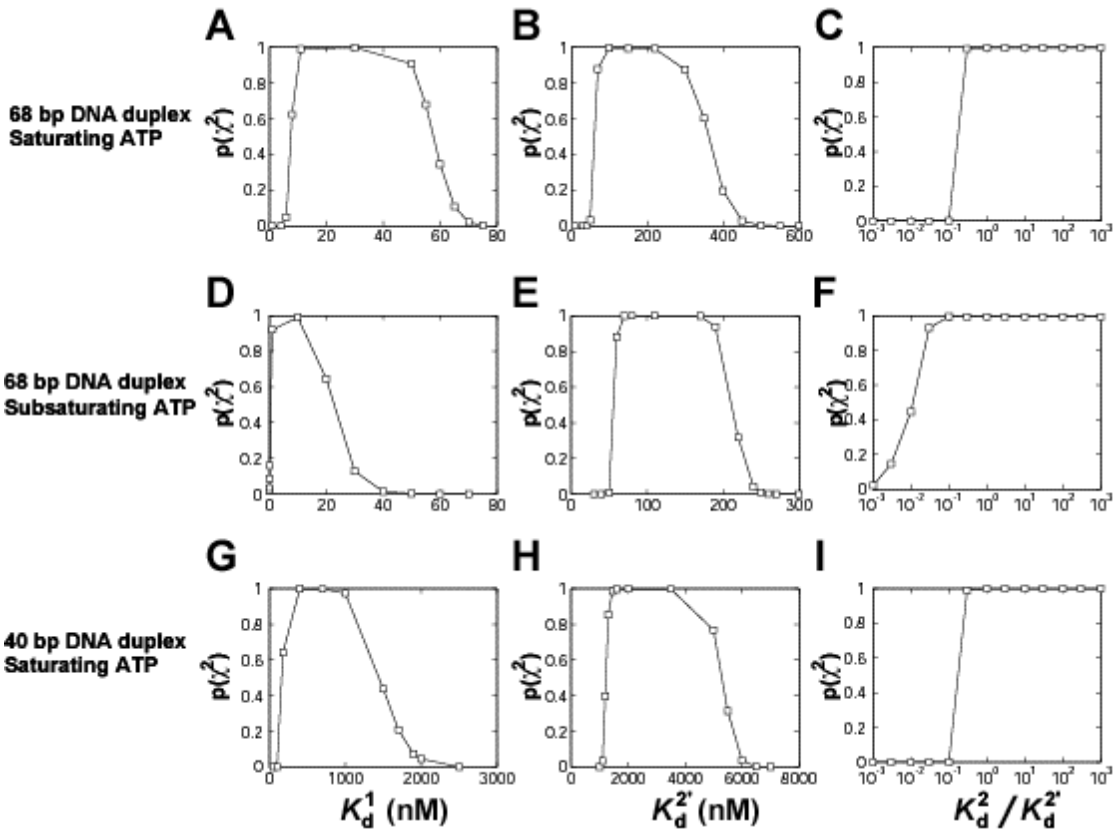

Supplementary Figure S3: Estimation of limits for K_d^1, $K_d^{2'}$ and $K_d^2 / K_d^{2'}$ (Scheme 1) for wild-type enzyme obtained from the DNA stimulation of the ATPase activity in Figure 2 and Supplementary Figure S4. The DNA stimulation curves of the ATPase activity using a 68 bp duplex under saturating (panels A, B and C), and subsaturating ATP concentrations (panels D, E and F) and the DNA stimulation curves using a 40 bp duplex under saturating ATP concentrations (panels G, H and I) were fit to models that systematically varied the indicated parameters, and the goodness of the fit for each model was estimated based on a χ^2 goodness-of-fits test. Values for the indicated parameters that give $p(\chi^2) \geq 0.05$ were considered acceptable and are summarized in Table II. In panels A, D and G, K_d^1 was systematically varied. $K_d^{2'}$ was varied in panels B, E, and H, and the degree of DNA binding cooperativity ($K_d^2 / K_d^{2'}$) was varied in panels C, F, and I. Partial ATPase stimulation of E^{DNA_1} and E_{DNA_2} compared to E was allowed in the fits as described in Supplementary Figure S2. As explained in Supplementary Figure S2, K_M^{ATP} values for E^{DNA_1} and E_{DNA_2} (Scheme 1) are not known but needed for the fits. In the fits shown it was postulated that E^{DNA_1} has the same K_M^{ATP} value as free enzyme (1 mM;

Table I) and that the $K_{\mathrm{M}}^{\mathrm{ATP}}$ for $\mathrm{E}_{\mathrm{DNA}_2}$ is the same as that for enzyme with saturating DNA (0.2 mM). Identical estimates of the acceptable values for the parameters analyzed in the Figure were obtained when different combinations of values for $K_{\mathrm{M}\{\mathrm{DNA}_1\}}^{\mathrm{ATP}}$ and $K_{\mathrm{M}\{\mathrm{DNA}_2\}}^{\mathrm{ATP}}$ were used as described in Supplementary Figure S2 ($K_{\mathrm{M}\{\mathrm{DNA}_1\}}^{\mathrm{ATP}} = K_{\mathrm{M}\{\mathrm{DNA}_2\}}^{\mathrm{ATP}} = 1$ mM, $K_{\mathrm{M}\{\mathrm{DNA}_1\}}^{\mathrm{ATP}} = 0.2$ mM and $K_{\mathrm{M}\{\mathrm{DNA}_2\}}^{\mathrm{ATP}} = 1$ mM, or $K_{\mathrm{M}\{\mathrm{DNA}_1\}}^{\mathrm{ATP}} = K_{\mathrm{M}\{\mathrm{DNA}_2\}}^{\mathrm{ATP}} = 0.2$ mM; analysis not shown).

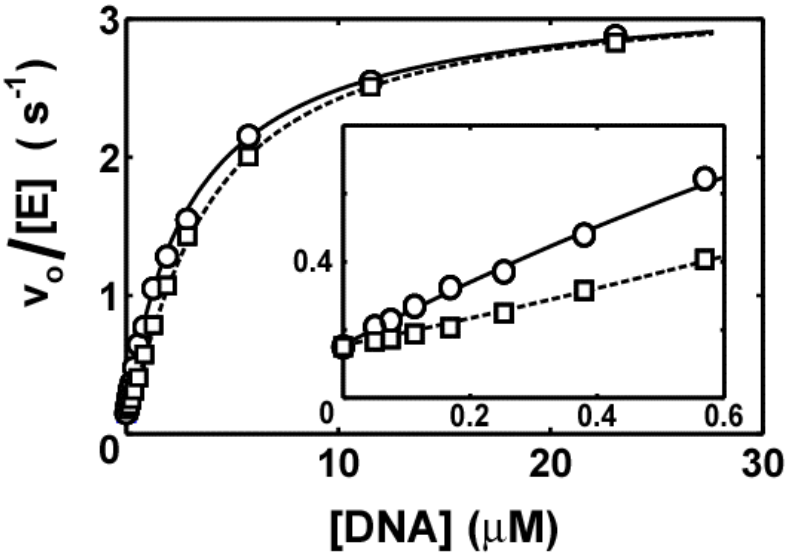

Supplementary Figure S4: ATPase stimulation by a 40 bp DNA duplex with saturating concentrations of Mg^{2+}-ATP (3 mM). A) Dependence of the observed ATP hydrolysis rate constant (v_o / [E]) on the DNA concentration with 13 nM (○) and 650 nM (□) topoisomerase II. Lines represent a global fit of Scheme 1 to the data.

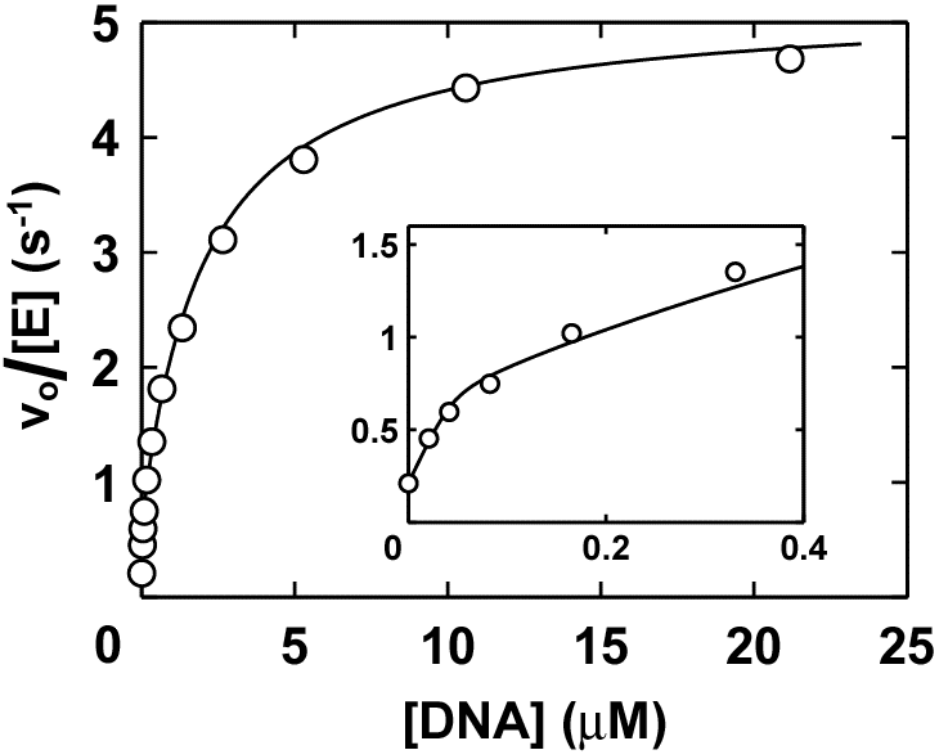

Supplementary Figure S5: Dependence of the observed ATP hydrolysis rate constant (v_o / [E]) of Y782F topoisomerase II (45 nM) on the concentration of the 68 bp DNA duplex with saturating (3 mM) Mg^{2+}-ATP. The line represents a fit of Scheme 1 to the data.

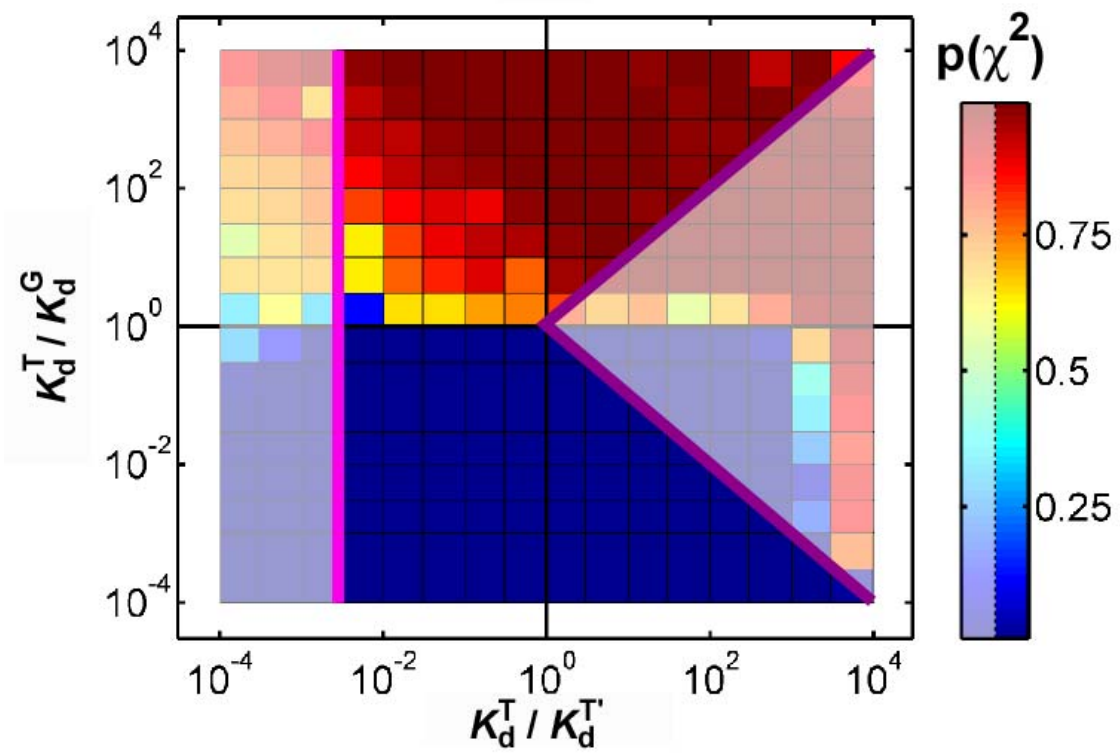

Supplementary Figure S6: Systematic search for models that are consistent with the DNA dependence of the ATPase activity and the topoisomerase II-mediated DNA cleavage with the side condition $K'_{clvg} \geq K_{clvg}$ (Scheme 2). Equilibrium cleavage data obtained at three enzyme concentrations [36 nM (data not shown), 360 nM and 3200 nM (Figure 4)] with varying concentrations of 46 bp duplexes in Mg^{2+}-AMPPNP were globally fit to models that varied in the amount of DNA binding cooperativity ($K_d^T / K_d^{T'}$) and in the relative affinities between the T- and the G-DNA sites (K_d^T / K_d^G). The goodness of the each fit p(χ^2) was estimated by χ^2 statistics. p(χ^2) (see color legend) was plotted on a two dimensional grid spanned by the ratios $K_d^T / K_d^{T'}$ and K_d^T / K_d^G. The area shown in saturated colors in between the magenta and violet lines represents combinations of values that are not ruled out based on the analysis of the DNA dependence of the ATPase reaction. Values located to the left of the magenta line ($K_d^T / K_d^{T'} < 3*10^{-3}$) possess a degree of negative DNA binding cooperativity that is not supported by the ATPase data (Supplementary Figure S3). Values to the right of the violet lines ($K_d^{T'} < K_d^G$ for

$K_d^T > K_d^G$ and $K_d^{G'} < K_d^T$ for $K_d^T < K_d^G$) are ruled out by the ATPase data as this area contains all values with positive, observed DNA binding cooperativity (Supplementary Figure S3 and Table II). The only values that are allowed by the results from the ATPase data (saturated colors) and that can fit the DNA cleavage data [$p(\chi^2) > 0.05$] are values for which the G-DNA site affinity exceeds that of the T-DNA site ($K_d^T / K_d^G > 10^0$).

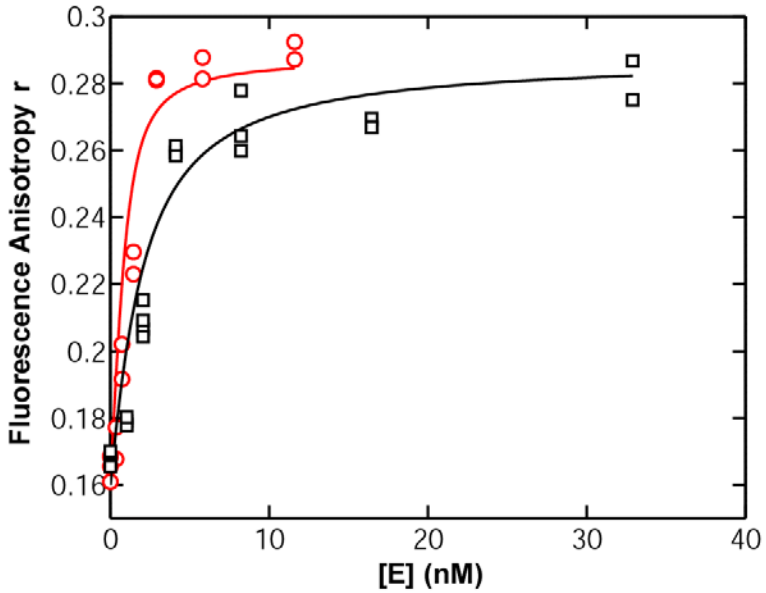

Supplementary Figure S7: Binding of ROX-labeled 40 bp DNA duplex (1 nM) to wild-type (black squares) or Y782F enzyme (red circles) in low salt buffer [25 mM Hepes-KOH pH 7.5, 5 mM $MgCl_2$, 50 mM KCl, 6% glycerol, 5 mM 2-mercaptoethanol]. Lines are fits of the data to the quadratic binding isotherm (Equation 1) to $K_d^{apparent}$ = 1.5 nM (black) and $K_d^{apparent}$ = 0.3 nM (red). However, these $K_d^{apparent}$ values only represent upper limits as the $K_d^{apparent}$ values are close to or lower than the DNA concentration used; i.e. the apparent binding curves represent stoichiometric titrations from which binding constants cannot be obtained.